Influence of Double Diffusive Effects on Miscible Viscous Fingering

M Mishra, P M J Trevelyan, C Almarcha, A de Wit

▶ **To cite this version:**

M Mishra, P M J Trevelyan, C Almarcha, A de Wit. Influence of Double Diffusive Effects on Miscible Viscous Fingering. Physical Review Letters, 2010, 105, 10.1103/physrevlett.105.204501 . hal-03566886

HAL Id: hal-03566886
https://hal.science/hal-03566886

Submitted on 11 Feb 2022

HAL is a multi-disciplinary open access archive for the deposit and dissemination of scientific research documents, whether they are published or not. The documents may come from teaching and research institutions in France or abroad, or from public or private research centers.

L'archive ouverte pluridisciplinaire **HAL**, est destinée au dépôt et à la diffusion de documents scientifiques de niveau recherche, publiés ou non, émanant des établissements d'enseignement et de recherche français ou étrangers, des laboratoires publics ou privés.

Influence of Double Diffusive Effects on Miscible Viscous Fingering

M. Mishra,[1,2] P. M. J. Trevelyan,[1] C. Almarcha,[1,3] and A. De Wit[1]

[1]*Nonlinear Physical Chemistry Unit and Center for Nonlinear Phenomena and Complex Systems, Faculté des Sciences, Université Libre de Bruxelles (ULB), CP231, 1050 Brussels, Belgium*

[2]*Department of Mathematics, Indian Institute of Technology Ropar, 140001 Rupnagar, India*

[3]*IRPHE, UMR 6594, CNRS, Université d'Aix-Marseille 1, 49, rue F. Joliot Curie, 13384 Marseille, France*

(Received 25 March 2010; published 8 November 2010)

Miscible viscous fingering classically occurs when a less viscous fluid displaces a miscible more viscous one in a porous medium. We analyze here how double diffusive effects between a slow diffusing S and a fast diffusing F component, both influencing the viscosity of the fluids at hand, affect such fingering, and, most importantly, can destabilize the classically stable situation of a more viscous fluid displacing a less viscous one. Various instability scenarios are classified in a parameter space spanned by the log-mobility ratios R_s and R_f of the slow and fast component, respectively, and parametrized by the ratio of diffusion coefficients δ. Numerical simulations of the full nonlinear problem confirm the existence of the predicted instability scenarios and highlight the influence of differential diffusion effects on the nonlinear fingering dynamics.

DOI: 10.1103/PhysRevLett.105.204501 PACS numbers: 47.20.Gv, 44.30.+v, 47.55.pd, 47.56.+r

Miscible viscous fingering (VF) occurs classically in porous media when a fluid of a given viscosity displaces another miscible more viscous fluid leading to a deformation of the corresponding interface into fingerlike patterns [1]. This paradigmatic pattern-forming instability has been the focus of numerous works devoted to study petroleum recovery [1], polymer processing [2], pollution spreading in soils [3] or efficiency of engineering separation techniques [3,4] to name a few. Except for some peculiar situations implying for instance Coriolis effects [5] or a surfactant-driven instability of a wetting layer [6], in all cases, VF is expected to occur only if the viscosity increases along the direction of propagation, the situation of a more viscous fluid displacing a less viscous one being classically understood as a stable situation. We show here that this intuitive picture is fundamentally modified if the fluid at hand contains two different components influencing the viscosity and diffusing at different rates.

Viscosity differences between miscible fluids can be related to temperature or composition changes and studies of such VF can be performed by analyzing displacements between two miscible solutions at different temperatures [7–14] or containing a viscosity changing solute in variable concentration [1–4]. In some cases, like in the displacement of oils by hot water [8] in enhanced oil recovery techniques, viscosity changes occur due to coupled thermal and solutal effects. As heat diffuses faster than mass, differential diffusion effects can influence the stability properties of VF patterns [9,13]. In parallel, there is also interest for miscible chemically driven VF [15–19] in which chemical reactions modify viscosity gradients. If the reaction is exothermic, viscosity changes are again possible due to both thermal and solutal effects [15]. Even in isothermal conditions, reactive systems typically involve several chemical species diffusing at different rates and which can influence the viscosity of the solution and hence affect stability with regard to VF [13]. The influence on nonlinear fingering of differential diffusion between two species both influencing the viscosity of a given solution, even in the absence of a reaction, remains however still unclear. The heat or mass problem and the two solutes one bear the similarity that, for both cases, the viscosity may depend on two scalars, say S and F, with one of them diffusing faster than the other one. Defining D_s and D_f as the diffusion coefficient of the, respectively, slow S and fast F species, it is of interest to understand how differential diffusion effects obtained when $\delta = D_f/D_s > 1$ can affect the problem.

In this context, this Letter discusses the generic influence on miscible VF of differential diffusion between two different scalars S and F each of them influencing independently the viscosity of a given solution. Using a quasisteady state approximation (QSSA), a time-dependent linear stability analysis (LSA) is performed to classify all possible VF instability scenarios in a parameter space spanned by the log-mobility ratio R_s and R_f of the, respectively, slow and fast diffusing species for variable values of the diffusion ratio δ. Differential diffusion effects are seen to destabilize in time a large part of the (R_s, R_f) parameter space otherwise stable when $\delta = 1$. We moreover highlight the influence of double diffusive effects on nonlinear fingering dynamics and suggest experimental conditions prone to demonstrate destabilization of a more viscous fluid pushing a less viscous one by differential diffusion. A discussion of similarities and differences between double-diffusion effects on VF with those classically known in buoyancy-driven flows [20] is conducted.

We consider a 2D horizontal porous medium or Hele-Shaw cell initially filled with a liquid solvent containing the scalars S and F in quantity S_2 and F_2 and of viscosity μ_2.

 © 2010 The American Physical Society

The same liquid solvent where the scalars are present with a value S_1 and F_1 giving a viscosity μ_1 is injected uniformly at an average velocity U in the longitudinal direction x. Following earlier studies [21], the viscosity is assumed to depend exponentially on the values S and F as $\mu = \mu_1 \exp[R_s(S - S_1)/(S_2 - S_1) + R_f(F - F_1)/(F_2 - F_1)]$ where μ_1 is the viscosity of the injected solution and $R_s = (S_2 - S_1)d(\ln\mu)/dS$ and $R_f = (F_2 - F_1)d(\ln\mu)/dF$. If $R_s > 0$, then for $R_f = 0$, we have $\mu_1 < \mu_2$ i.e. a less viscous solution of S displaces a more viscous one which is an unstable situation. If S stands for temperature, this would be the case of a hot fluid displacing a cold fluid for instance while if S stands for a viscosity increasing solute, this would correspond to a less concentrated solution of S displacing a more concentrated one. Similarly, $R_f > 0$ for $R_s = 0$ leads to instability with regard to the F component. When both S and F related effects are coupled and $\delta = 1$, the system is classically VF unstable when $\mu_1 < \mu_2$, i.e., $R_s + R_f > 0$. We seek here to obtain destabilization conditions for $R_s + R_f < 0$ when $\delta > 1$.

The evolution equations are Darcy's law and transport equations for S and F in a coordinate system moving at the injection speed U. Considering the characteristic length $L_c = D_s/U$ and time $t_c = D_s/U^2$, the scalar values S and F, pressure, velocity and viscosity are nondimensionalized as $\hat{s} = (S - S_1)/(S_2 - S_1)$, $\hat{f} = (F - F_1)/(F_2 - F_1)$, $\hat{p} = K(p - p_0)/(\mu_1 D_s)$, $\hat{\underline{u}} + \underline{i} = \underline{u}/U$ and $\mu = \hat{\mu}/\mu_1$, respectively, where p_0 is an arbitrary reference pressure. K is the permeability and $\underline{i}$ is the unit vector along x. Dropping hats for convenience, the dimensionless equations with $\nabla \cdot \underline{u} = 0$ are

$$\nabla p = -\mu(\underline{u} + \underline{i}), \tag{1a}$$

$$\mu = e^{R_s s + R_f f}, \tag{1b}$$

$$s_t + \underline{u} \cdot \nabla s = \nabla^2 s, \tag{1c}$$

$$f_t + \underline{u} \cdot \nabla f = \delta \nabla^2 f. \tag{1d}$$

In the absence of any transverse instabilities $\underline{u} = \underline{0}$, and the one-dimensional s, f, and viscosity base states are given analytically by $\bar{s} = \mathrm{erfc}(-x/2\sqrt{t})/2$, $\bar{f} = \mathrm{erfc}(-x/2\sqrt{\delta t})/2$, and $\bar{\mu} = \exp[R_s\bar{s} + R_f\bar{f}]$, where $x = 0$ is the initial interface position.

If $\delta = 1$, $\bar{s} = \bar{f}$, and $R_s + R_f > 0$ corresponds to a monotonically increasing $\bar{\mu}$, i.e., to the unstable situation, the reverse case $R_s + R_f < 0$ being stable. If $\delta > 1$, depending on the relative values of R_s and R_f, six different $\bar{\mu}$ profiles can be constructed (Fig. 1) [19,22] with differential diffusion effects triggering nonmonotonic viscosity profiles [23] in time in zones II, III, V, and VI. The boundaries of these various zones [13] can be found by noting that $\bar{\mu}_x$, the derivative of $\bar{\mu}$ with regard to x, changes sign at the two points satisfying $x^2 = \frac{4t\delta}{\delta - 1} \ln(-\sqrt{\delta}\frac{R_s}{R_f})$ which exist when $\sqrt{\delta}R_s/R_f < -1$. Further, the viscosity gradient at $x = 0$ is locally positive if and only if $\sqrt{\delta}R_s + R_f > 0$. Thus, a monotonically decreasing viscosity profile occurs when $R_f < \min(0, -\sqrt{\delta}R_s)$ which is region IV in Fig. 1. Although regions III and V are within the domain $R_s + R_f < 0$, they both have nonmonotonic viscosity profiles which could trigger VF instabilities locally in the zones where $\bar{\mu}_x > 0$.

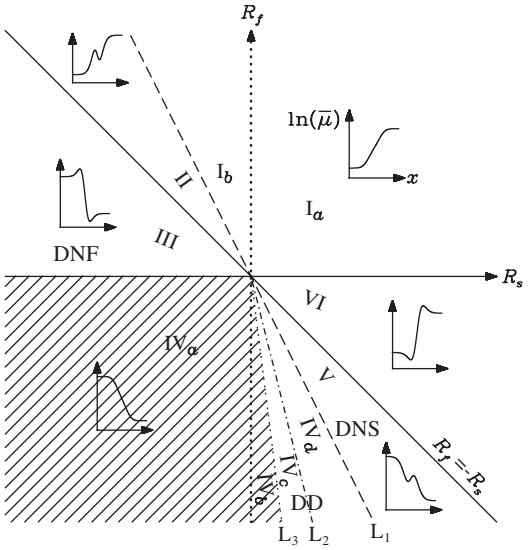

FIG. 1. Sketch in the (R_s, R_f) plane for $\delta > 1$ of the six different base state viscosity profiles $\bar{\mu}$, denoted by I–VI, where L_n $(n = 1, 2, 3)$ denotes the line $R_f = -\delta^{n/2}R_s$. Regions I_a, I_b, II, IV_d, V, and VI are initially unstable. Regions III and IV_c become unstable in the course of time. The two shaded regions IV_a and IV_b are always stable.

To understand how these nonmonotonic effects develop in time and more strikingly how instabilities can also be obtained in regions $IV_{c,d}$ where the viscosity decreases monotonically, a time-dependent LSA must be performed. At $t = 0$, the stability problem can be solved analytically to yield $R_s(1 - k/\sqrt{k^2 + \sigma}) + R_f(1 - k/\sqrt{k^2 + (\sigma/\delta)}) = 2\sigma/k$ where σ is the instantaneous growth rate for a disturbance of wave number k. This reveals that the system is stable at $t_0 = 0$ in regions III, $IV_{a,b,c}$ in Fig. 1 which is defined by $R_f < \min(-R_s, -\delta R_s)$ while it is right away unstable in IV_d and V. For $t_0 > 0$, the LSA is performed numerically using a QSSA [19,21]. As t_0 increases, the unstable regions expand across the (R_s, R_f) plane until in the large time asymptotic limit the only stable regions are $IV_{a,b}$ whose combined regions are defined by $R_f > \min(0, -\delta^{3/2}R_s)$. This condition predicts that region IV_c eventually becomes unstable in time while region IV_b remains stable. This suggests that, beyond destabilization due to the build-up of nonmonotonic viscosity profiles in time, differential diffusion is able to destabilize a monotonic increasing viscosity profile as is the case in zones $IV_{c,d}$.

To test these predictions and analyze the influence of differential diffusion on nonlinear fingering, we performed numerical simulations of the full nonlinear problem. A

stream function-vorticity formulation of Eq. (1) is solved using a pseudospectral method [24] on a 2D finite domain of size $L_x \times L_y$.

Figure 2 shows various VF cases for $R_s + R_f > 0$ and various δ i.e. for a globally less viscous fluid displacing a more viscous one. Figure 2(a) depicts classical VF for $\delta = 1$ occurring in quadrant I_a of Fig. 1 and characterized by tip splitting [1,24,25]. In this case, for a given constant λ, the resulting fingering pattern is the same for each point in the parameter space on the line $R_s + R_f = \lambda$. If now $\delta > 1$ in zone I_a, differential diffusion leads to a mushroom structured head as seen at the tip of the fingers in Fig. 2(b). The tip splitting mechanism is not observed any longer as the steep viscosity gradient at their origin is faded away by the faster diffusion of F. Clear mushroom structures in both forward and reverse fingers are observed in region I_b of Fig. 1, as shown in Figs. 2(c) and 2(d). For $R_f > 0$, an increase of δ at fixed (R_s, R_f) amplifies the extrema of the nonmonotonic change of μ transversely across the head of a finger [Figs. 2(e) and 2(f)] favoring the mushroom shape.

The most striking effect of differential diffusion is however to be able to destabilize the situation of a more viscous fluid pushing a less viscous one in the zone $R_s + R_f < 0$ (Figs. 3 and 4). Let us first examine the case when the contribution of the slow and fast diffusing scalars is, respectively, destabilizing and stabilizing, i.e., when $R_s > 0$ while $R_f < 0$. This corresponds for instance to cold water invading a hot enough viscous glycerol solution such that the global viscosity decreases along x. In region V of Fig. 1, the overall viscosity gradient is stable, however, a locally unstable zone develops in time across the interface as the fast diffusing component moves quickly towards the more viscous zone. Fingers grow around the interface in the zone where locally $\bar{\mu}_x > 0$; however, they eventually fade away far from it when they encounter the two stable zones where $\bar{\mu}_x < 0$ (Fig. 3, left). Fingers elongate more along the flow than against it [25] leading to an asymmetry in the pattern with regard to the initial position of the interface. This kind of destabilization, occurring in region V of Fig. 1, and due to a differential diffusion induced nonmonotonic viscosity profile when the slow component is destabilizing, will be referred to as DNS VF. However, such nonmonotonicity is not necessary for an instability as seen in Fig. 3 (right) where the associated base state viscosity profile is strictly monotonically decreasing (zone IV_d of Fig. 1). Such a destabilization referred to as double diffusive VF (DD VF) is due to a pure diffusive effect like in buoyancy-driven double-diffusion where fingers develop around a stable density profile when the slow (fast) diffusing species is destabilizing (stabilizing) [20].

We next examine the case when the fast diffusing scalar is the destabilizing component, the slow one being stabilizing, i.e., when $R_f > 0$ while $R_s < 0$ as is the case when a hot solution of glycerol invades cold water for instance. If $R_s + R_f < 0$ as in region III of Fig. 1, the base state viscosity profile consists of two locally unstable regions (one with a viscosity maximum, the other one with a minimum) developing in time at a symmetric increasing distance from the interface. This kind of destabilization, illustrated in Fig. 4, will be referred to as DNF-VF as here we have a differential diffusion induced nonmonotonic viscosity profile with the fast component being destabilizing. The interface where $\bar{\mu}_x < 0$ remains stable while VF

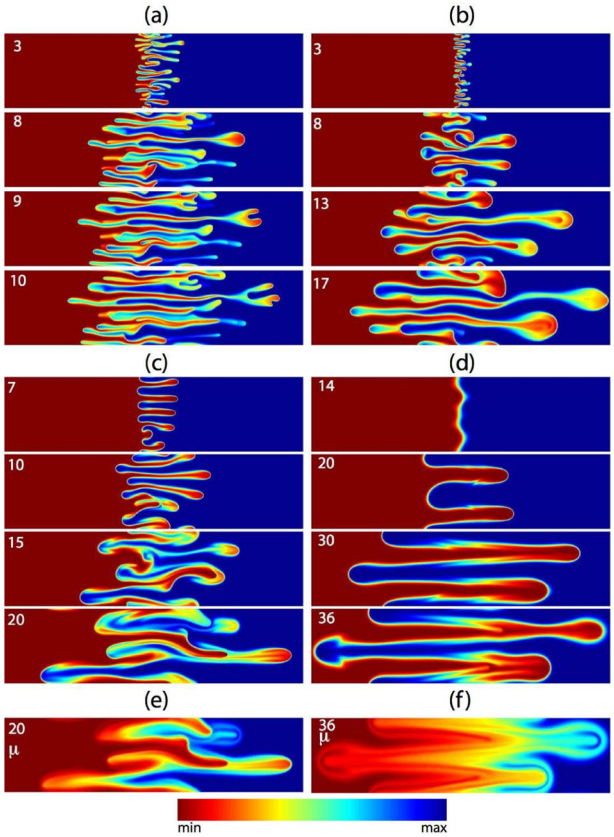

FIG. 2 (color online). Fingering dynamics of s for $L_y = 4096$ and $(R_s, R_f, \delta) =$ (a) (1,1,1), (b) (1,1,10), (c) $(-1, 3, 4)$, (d) $(-1, 3, 10)$. (e) and (f) are the viscosity fields corresponding to (c) and (d), respectively. The frame number is $t/10^3$.

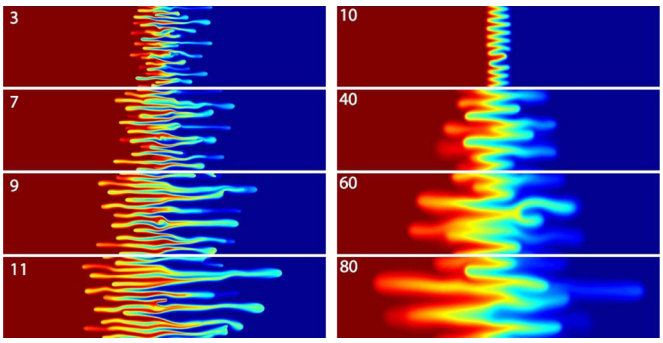

FIG. 3 (color online). Dynamics of s for (left) DNS VF, $R_s = 3$, $R_f = -3.6$, $\delta = 10$, $L_y = 4096$, (right) DD VF obtained for $R_s = 1$, $R_f = -3.2$, $\delta = 10$, $L_y = 2048$.

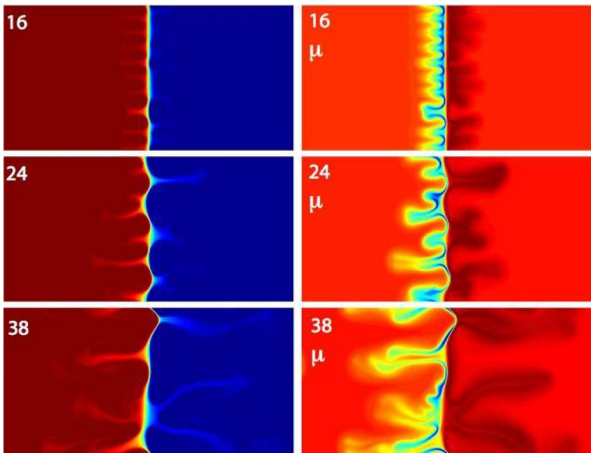

FIG. 4 (color online). DNF-VF dynamics of s (left) and of viscosity μ (right) for $R_s = -6.1$, $R_f = 6$, $\delta = 10$, $L_y = 8192$.

occurs in the two zones where $\bar{\mu}_x > 0$ at equal distances on either side of the interface. Forward fingers extend further than the reverse fingers as they develop along the flow while reverse fingers have to fight against it [25]. Here again, fingers have a mushroom type structure as $R_f > 0$. Such an instability is reminiscent of diffusive layer convection induced by buoyancy effects when a solution of the fast diffusing component overlies a denser solution of the slow species [26,27].

Although the mechanisms of DD, DNS, and DNF-VF triggered by differential diffusion bear similarities with those in buoyancy problems [20], there is a fundamental difference between them: buoyancy-driven patterns develop symmetrically around the unstable interface while in VF, triggered by a flow, asymmetric effects exist because fingers develop more easily along the flow than against it [25]. Analogous asymmetric effects can also be triggered by chemical reactions [27].

We have here studied how differential diffusion of two components each contributing to the viscosity of a solvent can profoundly affect the stability and nonlinear dynamics of viscous fingering. In the situation of a less viscous fluid pushing a more viscous one (i.e., when $R_s + R_f > 0$), double diffusion modifies the nonlinear dynamics and favors mushroom shaped fingers when the fast diffusing species is destabilizing. The most striking effects appear however when destabilization by differential diffusion of a more viscous fluid pushing a less viscous one is obtained. This occurs either due to the build-up in time of nonmonotonic viscosity profiles like in DNS (region V) or DNF (zone III) VF where locally unstable zones develop leading to spatially constrained nonlinear fingering. More interestingly, this also happens on a strictly monotonically decreasing viscosity profile (zone IV) because of a DD VF mechanism leading to smooth fingers. These various instability scenarios can be obtained by identifying the slow and fast component as mass and heat typically. Another way to experimentally look for the new instability scenarios predicted here is to use two nonreacting chemical species both influencing the viscosity of the solution but having sufficiently different diffusion coefficients. The wealth of available long chain molecules of variable length and thus tunable molecular weight and diffusion coefficients offers naturally to the experimentalist a tool kit to test the various proposed VF instability scenarios.

We thank Prodex and FNRS for financial support.

[1] G. M. Homsy, Annu. Rev. Fluid Mech. **19**, 271 (1987).
[2] K. V. McCloud and J. V. Maher, Phys. Rep. **260**, 139 (1995).
[3] A. De Wit, Y. Bertho, and M. Martin, Phys. Fluids **17**, 054114 (2005).
[4] W. De Malsche, J. Op De Beeck, H. Gardeniers, and G. Desmet, J. Chromatogr. A **1216**, 5511 (2009).
[5] J. A. Miranda and E. Alvarez-Lacalle, Phys. Rev. E **72**, 026306 (2005).
[6] C. K. Chan and N. Y. Liang, Phys. Rev. Lett. **79**, 4381 (1997).
[7] X. Kong, M. Haghighi, and Y. Yortsos, Fuel **71**, 1465 (1992).
[8] T. Sheorey and K. Muralidhar, Int. J. Thermal Sci. **42**, 665 (2003).
[9] D. Pritchard, J. Fluid Mech. **508**, 133 (2004).
[10] K. E. Holloway and J. R. de Bruyn, Can. J. Phys. **83**, 551 (2005); **84**, 273 (2006).
[11] M. N. Islam and J. Azaiez, Soc. Pet. Eng. J. 103243 (2006).
[12] Y. Nagatsu, N. Fujita, Y. Kato, and Y. Tada, Expt. Thermal Fluid Sci. **33**, 695 (2009).
[13] D. Pritchard, Eur. J. Mech. B, Fluids **28**, 564 (2009).
[14] M. N. Islam and J. Azaiez, Transp. Porous Media **84**, 821 (2010); **84**, 845 (2010).
[15] S. Swernath and S. Pushpavanam, J. Chem. Phys. **127**, 204701 (2007).
[16] Y. Nagatsu, K. Matsuda, Y. Kato, and Y. Tada, J. Fluid Mech. **571**, 475 (2007).
[17] T. Podgorski, M. Sostarecz, S. Zorman, and A. Belmonte, Phys. Rev. E **76**, 016202 (2007).
[18] T. Gérard and A. De Wit, Phys. Rev. E **79**, 016308 (2009).
[19] S. H. Hejazi, P. M. J. Trevelyan, J. Azaiez, and A. De Wit, J. Fluid Mech. **652**, 501 (2010).
[20] J. S. Turner, *Buoyancy Effects in Fluids* (Cambridge University Press, Cambridge, England, 1979).
[21] C. T. Tan and G. M. Homsy, Phys. Fluids **29**, 3549 (1986).
[22] L. Rongy, P. M. J. Trevelyan, and A. De Wit, Phys. Rev. Lett. **101**, 084503 (2008).
[23] O. Manickam and G. M. Homsy, Phys. Fluids **6**, 95 (1994).
[24] C. T. Tan and G. M. Homsy, Phys. Fluids **31**, 1330 (1988).
[25] M. Mishra, M. Martin, and A. De Wit, Phys. Rev. E **78**, 066306 (2008).
[26] R. W. Griffiths, J. Fluid Mech. **102**, 221 (1981).
[27] C. Almarcha, P. M. J. Trevelyan, P. Grosfils, and A. De Wit, Phys. Rev. Lett. **104**, 044501 (2010).